The rotational spectrum of rhomboidal SiC 3

A. J. Apponi, M. C. McCarthy, C. A. Gottlieb, and P. Thaddeus

Citation: The Journal of Chemical Physics **111**, 3911 (1999); doi: 10.1063/1.479694
View online: http://dx.doi.org/10.1063/1.479694
View Table of Contents: http://scitation.aip.org/content/aip/journal/jcp/111/9?ver=pdfcov
Published by the AIP Publishing

The rotational spectrum of rhomboidal SiC_3

A. J. Apponi, M. C. McCarthy, C. A. Gottlieb, and P. Thaddeus
Harvard-Smithsonian Center for Astrophysics, Cambridge, Massachusetts 02138 and Division of Engineering and Applied Sciences, Harvard University, Cambridge, Massachusetts 02138

(Received 22 April 1999; accepted 12 May 1999)

Rhomboidal SiC_3, a planar ring with C_{2v} symmetry and a transannular C–C bond, was detected at centimeter wavelengths in a pulsed supersonic molecular beam with a Fourier transform microwave (FTM) spectrometer, and was subsequently observed in a low-pressure dc glow discharge with a free-space millimeter-wave absorption spectrometer. The rotational spectrum of SiC_3 is characterized by large harmonic defects and large splitting of the *K*-type doublets. Lines in the centimeter-wave band were very strong, allowing the singly substituted isotopic species to be observed in natural abundance. Measurements of the normal and five isotopically substituted species with the FTM spectrometer provided conclusive evidence for the identification and yielded an experimental zero-point (r_0) structure. Forty-six transitions between 11 and 286 GHz with $K_a \leqslant 6$ were measured in the main isotopic species. Three rotational and nine centrifugal distortion constants in Watson's *A*-reduced Hamiltonian reproduce the observed spectrum to within a few parts in 10^7 and allow the most intense transitions up to 300 GHz to be calculated with high accuracy. The spectroscopic constants confirm that SiC_3 is a fairly rigid molecule: the inertial defect is comparable to those of well-known planar rings and the centrifugal distortion constants are comparable to molecules of similar size. The number of SiC_3 molecules in our supersonic molecular beam in each gas pulse is at least 3×10^{11}, so large that electronic transitions may be readily detectable by laser spectroscopy. © *1999 American Institute of Physics.*
[S0021-9606(99)00330-X]

I. INTRODUCTION

Silicon tricarbide (SiC_3), the long-predicted planar ring with a transannular bond shown in Fig. 1, has been detected,[1] and its geometrical structure and radio spectrum determined to high precision. On the basis of the laboratory rest frequencies, seven lines of SiC_3 were soon identified with a radio telescope in the expanding envelope of IRC+10 216, establishing this highly polar and reactive rhomboidal ring as the fifth and largest cyclic molecule in space.[2] Here, we give a detailed account of the laboratory work, including (i) derivation of the geometrical structure by isotopic substitution, (ii) measurement and analysis of the small spin-rotation hyperfine structure observed at high resolution in those isotopic species with nuclear magnetic moments, (iii) detailed characterization of the centrifugal distortion of the molecule to the top of the radio band, and (iv) tabulation of those rotational lines in the radio band which are likely to be of the greatest laboratory and astronomical interest.

II. EXPERIMENT

A. Centimeter-wave measurements

Rhomboidal SiC_3 was first detected with a Fourier transform microwave (FTM) spectrometer, an instrument that for the work here operated between about 6 and 26 GHz (Ref. 3). Reactive molecules are produced in a small electric discharge in the throat of a nozzle through a stream of precursor gases heavily diluted in Ne or Ar, just prior to supersonic expansion to about Mach 2 in a large vacuum chamber. The strongest lines of SiC_3 were observed with source conditions similar to those that optimize lines of the known silicon molecules SiC_2 and SiC_4: a mixture of silane (SiH_4; 0.1%) and diacetylene (HC_4H; 0.2%) diluted in Ne, a stagnation pressure behind the pulsed valve of 3.5 atm, a discharge potential of 1100 V, and a gas pulse 140 μs long. Under these conditions, lines of SiC_3 were observed with a signal-to-noise ratio of 400 or greater in 1 min of integration, as the sample spectrum in Fig. 2(a) illustrates.

Following the detection of the two lowest rotational transitions of the normal isotopic species (i.e., $^{28}Si^{12}C_3$), the corresponding transitions of the rare isotopic species with ^{29}Si, ^{30}Si, and ^{13}C were observed in natural abundance at precisely the expected frequency shifts. An additional isotopic species, that with disubstituted off-axis carbon-13, was detected by adding carbon-13-enriched CO (99.1% ^{13}C; Isotec) to the precursor gas. Detection of all four rare isotopic species of SiC_3 in natural abundance, and magnetic hyperfine structure (hfs) in the ^{29}Si [Fig. 2(b)] and ^{13}C species, demonstrate the high sensitivity of our FTM spectrometer and the high yield of SiC_3 in our discharge source. In contrast to the fairly weak lines of the normal species observed with the millimeter-wave spectrometer (Sec. III B), the rare isotopic species were detected with integration times of only 1 to 2 min per line.

Considerable care was taken to demonstrate that rhomboidal SiC_3 is the carrier of the assigned lines. The extensive isotopic measurements summarized in Table I constitute nearly conclusive evidence for the identification. It was also shown that (i) none of the lines attributed to SiC_3 exhibits a

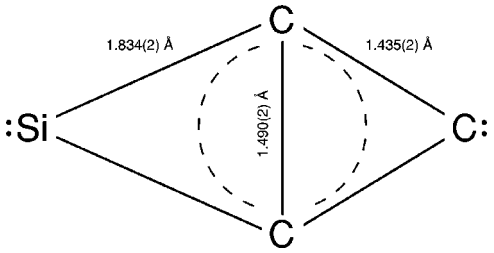

FIG. 1. Structure of rhomboidal SiC_3 that best reproduces the observed rotational transitions of 6 isotopic species (see Sec. IV A).

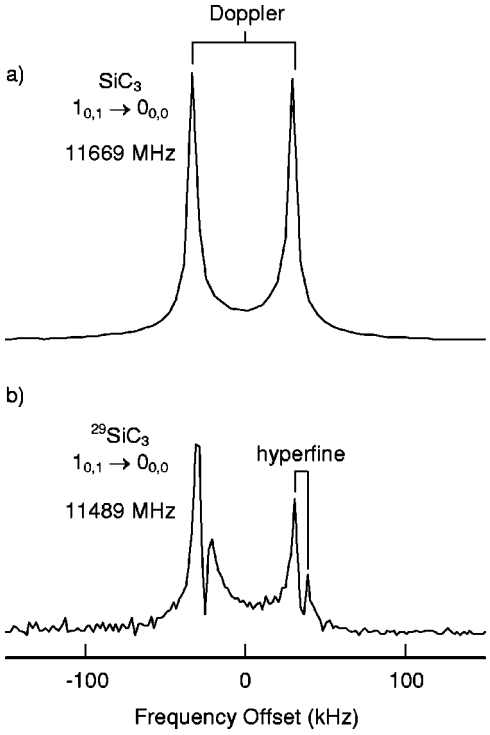

FIG. 2. Sample FTM spectra of the fundamental, $J_{K_a,K_c}=1_{0,1}-0_{0,0}$ transition of SiC_3. (a) The normal isotopic species showing the double-peaked line profile resulting from the interaction of the Mach 2 supersonic molecular beam with the two traveling waves of the confocal Fabry–Perot mode. (b) The rare isotopic species $^{29}SiC_3$ observed in natural abundance, the resolved hyperfine structure resulting from the nuclear spin-rotation ($\mathbf{I}\cdot\mathbf{J}$) interaction. Each spectrum was observed with an integration time of 1 min.

detectable Zeeman effect, as expected for a molecule with a closed-shell $^1A_1$ electronic ground state, (ii) the lines vanish when either the discharge is turned off or silane is absent, as expected for a reactive silicon-bearing molecule, (iii) no lines were found at subharmonic frequencies, confirming the assigned rotational quantum numbers, (iv) the intensities of the isotopic lines are about those expected, both in natural abundance or with carbon-13 enrichment, and (v) magnetic $\mathbf{I}\cdot\mathbf{J}$ hfs exists as expected in those isotopic species with nuclear spin.

The abundance of SiC_3 in the molecular beam was estimated by comparing the line intensities with those of the rare isotopic species of OCS observed in a discharge-free beam of 1% OCS in Ne. We estimate that there are $\geqslant 3\times10^{11}$ SiC_3 molecules per gas pulse, on the assumption that all the molecules are in the active region of the microwave cavity.

B. Millimeter-wave measurements

The millimeter-wave rotational spectrum of SiC_3 was measured in absorption with a free-space spectrometer that operates between 70 and 400 GHz.[4,5] Silicon–carbon clusters are produced in a low-pressure dc discharge through a flowing mixture of SiH_4, HCCH, and Ar in the approximate molar ratio of 12:6:1. The flow rate of SiH_4 at standard temperature and pressure (STP) was 12 cm^3/min and the total pressure in the cell with the discharge on was about 35 mTorr. The strongest lines were observed with a fairly high discharge current of 0.75 A at a potential of 1300 V; sensitivity enhancement by about a factor of 20 was achieved by cooling the large glass discharge cell (300 cm long, 15 cm in diameter) to about 150 K. Under these conditions, lines of SiC_3 are about 25 times weaker than those of SiC_2 (Ref. 6) and 5 times weaker than those of SiC (Ref. 7). The concentration of SiC_3 ($\sim 2\times10^{10}$ cm^{-3}), corresponding to a mole fraction of approximately 1×10^{-5} (for an assumed dipole moment of 4.2 D; Ref. 8), is about a factor of 3 less than that of SiC_2.

Silane is spontaneously flammable in air at concentrations of 5% or more,[9] and its by-products in a discharge include abrasive solids like silicon dioxide and carborundum that are damaging to mechanical vacuum pumps. In the FTM experiment, no special precautions were taken because of the heavy dilution and the low flow rate of SiH_4, but in the millimeter-wave experiment the flow rate was about 500 times higher and the gas was only slightly diluted. Care was therefore required to dispose properly of the unreacted silane and its discharge products. The exhaust from the discharge cell was first passed through a 1 in. diameter stainless-steel pipe in a tube furnace 33 cm long heated to about 600 °C, a temperature at which silane decomposes rapidly to Si and H_2

TABLE I. Microwave transitions of SiC_3 isotopic species.[a]

$J'_{K'_a,K'_c}\rightarrow J_{K_a,K_c}$	SiCCC	^{29}SiCCC	^{30}SiCCC	SiCC^{13}C on-axis	Si^{13}CCC off-axis	Si^{13}C^{13}CC off-axis
$1_{0,1}\rightarrow 0_{0,0}$	11 669.767	11 489.337[b]	11 320.030	11 283.126[b]	11 605.327[b]	11 542.089
$2_{0,2}\rightarrow 1_{0,1}$	23 320.745	22 961.058	22 623.495	22 549.923[b]	23 189.834[b]	23 061.086
$2_{1,2}\rightarrow 1_{1,1}$					22 288.662[b]	22 135.539[b]
$2_{1,1}\rightarrow 1_{1,0}$					24 132.513[b]	24 032.672[b]

[a]Estimated measurement uncertainty: 1 kHz.
[b]Centroid of hyperfine split line.

(Ref. 9). To ensure that the pump was not damaged by particles swept from the furnace by the gas stream, a multistage vacuum inlet trap (with charcoal and two micron filters) was installed between the furnace and pump, and the pump oil was continuously circulated through an oil filtration system with two micron filters (VISI-flow). Finally, inert gas was added at a point close to the pump outlet to ensure that if SiH_4 did reach the exhaust system (which was entirely metallic), it was sufficiently dilute to avoid spontaneous combustion when it came into contact with air.

III. OBSERVED SPECTRA

A. FTM spectrum

Rhomboidal SiC_3 is a prolate asymmetric top ($\kappa = -0.945$) with C_{2v} symmetry and *a*-type rotational transitions, sufficiently close to the symmetric top limit ($\kappa = -1$) that K_a is nearly a good quantum number, and can be abbreviated to K. Owing to the two equivalent off-axis carbon nuclei (Fig. 1), Bose–Einstein statistics restrict K to even integers in the normal isotopic species, but K is both odd and even if one or both atoms which lie off the symmetry axis (hereafter referred to as the ''off-axis'' carbon atoms) are ^{13}C. A further consequence of the two off-axis carbon atoms is that the difference between the B and C rotational constants is large and the harmonic defect, which is proportional to $(B-C)^2/\{8[A-(B+C)/2]\}$ in the $K=0$ ladder, is roughly 500 times greater than the leading centrifugal distortion term $4\Delta_J$.

Only two transitions of the main isotopic species of SiC_3 were accessible with the FTM spectrometer, both in the $K=0$ rotational ladder: the fundamental $J=1-0$ transition and its approximate first harmonic, the $2-1$ transition. The first transition was tentatively identified in a wideband frequency survey near 11.7 GHz, and the $2-1$ transition then identified at 23.3 GHz at the expected relative intensity (Table I). The observed harmonic defect, $2\nu_{10}-\nu_{21}=18.8$ MHz, was very close to the 19.9 MHz predicted from the theoretical structure,[8] providing the first indication that McCarthy *et al.*[1] had detected SiC_3. Owing to the large harmonic defect, the FTM measurement of the two $K=0$ lines yielded initial values of $(B+C)$ and $(B-C)$ on the assumption that the A rotational constant was the value calculated from the theoretical structure. Following the identification of the normal isotopic species, all accessible transitions were measured in the singly substituted isotopic species, as well as those of the disubstituted off-axis ^{13}C species. The two $K=1$ lines in the off-axis ^{13}C species yielded a direct determination of $(B+C)$ and $(B-C)$, an initial estimate of A from the harmonic defect, and one centrifugal distortion constant (Δ_{JK}). The measured hfs and principal elements of the nuclear spin-rotation tensor for the ^{29}Si and singly substituted ^{13}C species are given in Table II.

The sensitivity of our FTM spectrometer was crucial for the identification and structural determination of rhomboidal SiC_3, but owing to the limited frequency range of this instrument, the centrifugal distortion terms required to calculate the spectrum at high frequencies could not be determined. For that, it was necessary to extend the measurements into the millimeter-wave band.

TABLE II. Observed hfs of SiC_3 isotopic species.[a,b]

$J'_{K'_a,K'_c} \rightarrow J_{K_a,K_c}$ $F' \rightarrow F$	$^{29}SiCCC$	$SiCC^{13}C$ on-axis	$Si^{13}CCC$ off-axis	$Si^{13}C^{13}CC$ off-axis
$1_{0,1} \rightarrow 0_{0,0}$				
$3/2 \rightarrow 1/2$	−3.2	+6.0	+1.6	0
$1/2 \rightarrow 1/2$	+6.4	−3.0	−3.2	0
$2_{0,2} \rightarrow 1_{0,1}$				
$5/2 \rightarrow 3/2$	0	+2.1		0
$3/2 \rightarrow 1/2$	0	−3.7		0
$2_{1,2} \rightarrow 1_{1,1}$				
$5/2 \rightarrow 3/2$			−4.2	
$3/2 \rightarrow 1/2$			+7.4	
$3 \rightarrow 2$				−6.1
$2 \rightarrow 1$				+11.2
$2_{1,1} \rightarrow 1_{1,0}$				
$5/2 \rightarrow 3/2$			−3.5	
$3/2 \rightarrow 1/2$			+6.2	
$3 \rightarrow 2$				−5.0
$2 \rightarrow 1$				+9.3

[a]Estimated measurement uncertainty: 1 kHz.

[b]Nuclear spin-rotation tensor elements in kHz: $N_{aa}=43(4)$, $N_{bb}=4(1)$ and $N_{cc}=2(1)$ for off-axis ^{13}C; $(N_{bb}+N_{cc})=-13(1)$ for on-axis ^{29}Si; and $(N_{bb}+N_{cc})=12(1)$ for on-axis ^{13}C. The tensor elements differ slightly from those in Ref. 1, owing to the higher accuracy of the measured hfs.

B. Millimeter-wave spectrum

Soon after SiC_2 was detected in the laboratory at millimeter wavelengths,[6] an extensive search for SiC_3 was undertaken, but was unsuccessful owing to the uncertainties in frequencies calculated from the theoretical structures and the large number of unassigned background lines. Following the FTM measurements, a new search for SiC_3 in the millimeter-wave band was undertaken. The FTM measurements allowed us to restrict the search range, thereby reducing the number of candidate lines that had to be subjected to tedious assays and harmonic frequency checks. As before, many background lines were present, but only one or two were shown to contain silicon within the restricted search range of ~200 MHz.

Five lines with approximately the same intensity were tentatively assigned to SiC_3 on the basis of the close agreement to $K=0$ transitions calculated with four spectroscopic constants (A,B,C, and Δ_J) derived from the FTM measurements. With slight adjustments to the constants in this highly truncated Hamiltonian, the two microwave transitions and the five high frequency lines between 145 and 221 GHz were fit to within the measurement uncertainties, confirming the assignment of the millimeter-wave lines. Using these constants and Δ_{JK} from the off-axis ^{13}C species, lines in the $K=2$ ladder were soon identified; as more spectroscopic constants were determined, lines in the $K=4$ and 6 ladders were assigned as well.

In all, 46 *a*-type *R*-branch ($\Delta J=1$) transitions in the $K=0,2,4$, and 6 rotational ladders were measured (Table III). Only $\Delta K=0$ transitions were observed in SiC_3, because the $\Delta K=2$ cross-ladder transitions are predicted to be more than 100 times weaker than the $\Delta K=0$ transitions, and hence are

TABLE III. Measured rotational frequencies of SiC_3.[a]

Transition J_{K_a,K_c} upper–lower	Measured frequencies (MHz)	$O-C$ (kHz)	S	E/k (K)
$1_{0,1}\rightarrow 0_{0,0}$	11 669.767±0.001	1	1.0	0.6
$2_{0,2}\rightarrow 1_{0,1}$	23 320.745±0.001	2	2.0	1.7
$9_{0,9}\leftarrow 8_{0,8}$	102 916.155±0.015	23	8.9	24.9
$12_{0,12}\leftarrow 11_{0,11}$	135 552.648±0.013	15	11.9	42.9
$13_{0,13}\leftarrow 12_{0,12}$	146 294.449±0.016	−14	12.9	49.9
$14_{0,14}\leftarrow 13_{0,13}$	156 999.642±0.012	−13	13.9	57.4
$14_{2,13}\leftarrow 13_{2,12}$	162 016.877±0.013	7	13.7	64.7
$14_{4,10}\leftarrow 13_{4,9}$	163 999.747±0.022	−77	12.8	83.6
$15_{0,15}\leftarrow 14_{0,14}$	167 684.637±0.010	1	14.9	65.4
$14_{2,12}\leftarrow 13_{2,11}$	168 324.911±0.018	−39	13.7	66.1
$15_{2,14}\leftarrow 14_{2,13}$	173 372.071±0.011	−18	14.7	73.0
$15_{4,12}\leftarrow 14_{4,11}$	175 735.759±0.013	60	13.9	92.0
$15_{4,11}\leftarrow 14_{4,10}$	175 818.135±0.013	−22	13.9	92.0
$15_{2,13}\leftarrow 14_{2,12}$	180 628.926±0.016	−30	14.7	74.8
$16_{2,15}\leftarrow 15_{2,14}$	184 686.224±0.011	−7	15.7	81.9
$17_{0,17}\leftarrow 16_{0,16}$	189 040.562±0.011	−8	16.9	83.1
$16_{2,14}\leftarrow 15_{2,13}$	192 883.465±0.013	−22	15.7	84.0
$18_{0,18}\leftarrow 17_{0,17}$	199 725.499±0.017	−21	17.9	92.7
$19_{2,18}\leftarrow 18_{2,17}$	218 374.960±0.013	−14	18.7	111.7
$19_{4,15}\leftarrow 18_{4,14}$	223 411.104±0.031	−19	18.1	131.5
$19_{2,17}\leftarrow 18_{2,16}$	229 210.868±0.093	42	18.8	115.3
$21_{0,21}\leftarrow 20_{0,20}$	231 837.216±0.021	−11	20.9	124.5
$20_{4,17}\leftarrow 19_{4,16}$	234 818.044±0.015	9	19.2	142.7
$20_{4,16}\leftarrow 19_{4,15}$	235 417.188±0.013	−19	19.2	142.8
$21_{2,20}\leftarrow 20_{2,19}$	240 624.286±0.013	12	20.7	134.3
$20_{2,18}\leftarrow 19_{2,17}$	241 138.145±0.014	90	19.8	126.8
$22_{0,22}\leftarrow 21_{0,21}$	242 559.685±0.033	4	21.9	136.2
$21_{4,18}\leftarrow 20_{4,17}$	246 650.400±0.013	2	20.2	154.5
$21_{4,17}\leftarrow 20_{4,16}$	247 480.048±0.016	2	20.2	154.6
$23_{0,23}\leftarrow 22_{0,22}$	253 289.776±0.067	41	22.9	148.3
$22_{6,17}\leftarrow 21_{6,16}$	257 675.781±0.050	39	20.3	197.4
$22_{6,16}\leftarrow 21_{6,15}$	257 678.641±0.050	−139	20.3	197.4
$22_{4,19}\leftarrow 21_{4,18}$	258 481.070±0.015	8	21.2	166.9
$22_{4,18}\leftarrow 21_{4,17}$	259 607.172±0.015	−4	21.2	167.1
$23_{2,22}\leftarrow 22_{2,21}$	262 716.484±0.014	29	22.7	159.0
$24_{0,24}\leftarrow 23_{0,23}$	264 026.154±0.018	12	23.9	161.0
$22_{2,20}\leftarrow 21_{2,19}$	264 663.579±0.016	−79	21.8	151.7
$23_{6,18}\leftarrow 22_{6,17}$	269 474.594±0.050	11	21.4	210.4
$23_{6,17}\leftarrow 22_{6,16}$	269 479.625±0.050	65	21.4	210.4
$23_{4,20}\leftarrow 22_{4,19}$	270 306.122±0.013	−5	22.3	179.9
$23_{4,19}\leftarrow 22_{4,18}$	271 805.866±0.016	1	22.3	180.1
$24_{2,23}\leftarrow 23_{2,22}$	273 708.692±0.015	−21	23.7	172.1
$25_{0,25}\leftarrow 24_{0,24}$	274 767.728±0.018	18	24.9	174.2
$24_{4,21}\leftarrow 23_{4,20}$	282 121.343±0.019	−14	23.3	193.4
$24_{4,20}\leftarrow 23_{4,19}$	284 082.408±0.023	42	23.3	193.8
$26_{0,26}\leftarrow 25_{0,25}$	285 513.302±0.018	−65	25.9	187.9

[a]The two lowest transitions at centimeter wavelengths were measured with the FTM spectrometer; the high-frequency transitions were measured with the free-space millimeter-wave absorption spectrometer. S is the asymmetric rotor line strength. E/k is the energy of the upper level of the transition.

below the detection sensitivity. A typical millimeter-wave spectrum of a $K=0$ transition is shown in Fig. 3(a), while Fig. 3(b) illustrates the large asymmetry splitting in a $K=6$ transition near 258 GHz. Owing to the greater widths of the predominately pressure-broadened millimeter-wave lines [1–1.5 MHz full width at half maximum (FWHM)], the fractional measurement uncertainties are higher than those of the centimeter-wave lines.

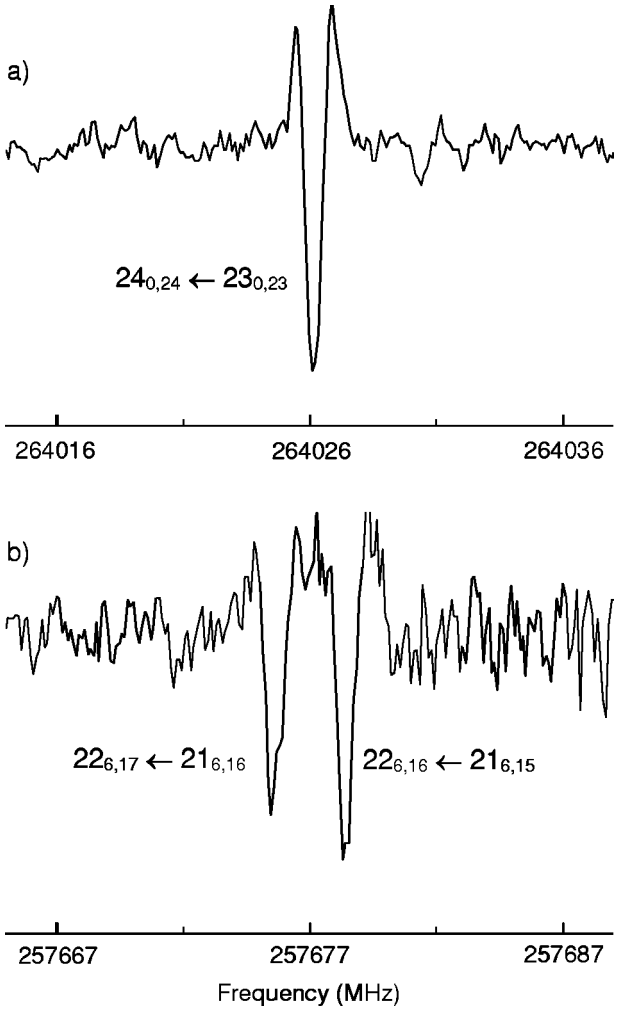

FIG. 3. Sample millimeter-wave absorption spectra of SiC_3, each the result of an integration time of ~10 min. (a) The $24_{0,24}\leftarrow 23_{0,23}$ line near 264 GHz and (b) the $22_6\leftarrow 21_6$ doublet near 258 GHz. The instrumental line shape is approximately the second derivative of a Lorentzian, owing to the modulation scheme employed.

IV. SPECTROSCOPIC ANALYSIS

The transition frequencies in Table III were analyzed with Watson's A-reduced Hamiltonian. With 12 spectroscopic constants, this Hamiltonian fits the observed lines to an rms uncertainty (39 kHz) that is comparable to that of other reactive molecules observed in the millimeter-wave band[10]—i.e., to within about 4% of the pressure-broadened linewidth. In the final fit (Table IV), the fourth-order centrifugal distortion constant Δ_K was constrained to zero owing to the high correlation with the A rotational constant: the only significant correlation (0.96) is between the distortion constants Δ_J and Φ_J. In an attempt to obtain a better estimate of the uncertainty in A, we tried varying Δ_K. To within the statistical uncertainties, A has essentially the same value when Δ_K is included in the fit, but the correlations between the spectroscopic constants are much greater and the rms of the fit is only slightly smaller. A better determination of the A rotational constant will require measurement of $\Delta K=2$ cross-ladder transitions.

The rotational constants of the on-axis isotopic species

TABLE IV. Spectroscopic constants of SiC_3.

Constant[a]	Measured[b]	Expected
Rotational constants:		
A	37 943.76(51)	39044[c]
B	6 282.904(4)	6279[c]
C	5 386.868(4)	5409[c]
Quartic centrifugal distortion constants:		
$\Delta_J\times10^3$	1.667(4)	
$\Delta_{JK}\times10^3$	8.55(12)	
Δ_K	0.0[d]	
$\delta_J\times10^3$	0.229(5)	
$\delta_K\times10^3$	10.3(5)	
Sextic centrifugal distortion constants:		
$\Phi_J\times10^6$	-0.020(5)	
$\Phi_{JK}\times10^6$	−1.88(25)	
$\Phi_{KJ}\times10^6$	61.0(64)	
$\phi_J\times10^6$	−0.026(3)	
$\phi_{JK}\times10^6$	−2.7(5)	
Inertial defect (amu Å^2):		
Δ	0.060 52(17)	(0.04−0.10)[e]

[a]Rotational and centrifugal distortion constants in MHz. Uncertainties (1σ) are in units of the last significant digit.
[b]Derived from a least-squares fit of Watson's A-reduced Hamiltonian to the data in Table III.
[c]From an *ab initio* calculation at the DZP CISD level of theory (Ref. 8).
[d]Constrained to zero because of the high correlation with A.
[e]Range of the inertial defect in 10 planar rings (Ref. 12).

measured with the FTM spectrometer were initially derived on the assumption that the inertial defect ($\Delta = I_C - I_A - I_B$) is the same as that of the off-axis ^{13}C species, but the inertial defect of the normal species determined from the combined centimeter- and millimeter-wave measurements (Table IV) is approximately 10% smaller than in the off-axis ^{13}C species (Table V). Following the analysis of the entire set of measurements for the normal species, the rotational constants of the on-axis rare isotopic species were reanalyzed with A and Δ_J constrained to the values determined for the normal species (Table V).

At the start of this investigation, there was considerable uncertainty as to the rigidity of SiC_3. In SiC_2, the inertial defect (0.36) and the leading centrifugal distortion constants are large; many higher-order terms in the standard Hamiltonian for an asymmetric top with centrifugal distortion are needed to describe the millimeter-wave spectrum.[6] Subsequent experimental and theoretical investigations of SiC_2 showed that there is a large-amplitude vibration which accounts for the anomalous centrifugal distortion constants and large inertial defect (Ref. 11 and references therein).

The present spectroscopic measurements establish that rhomboidal SiC_3 is planar, has C_{2v} symmetry, and is fairly rigid. Planarity of the four-membered ring is established from the small positive inertial defect (0.06) which lies within the range of 10 well-known planar rings such as furan (0.046), pyrrole (0.076), pyridene (0.039), etc.[12] The symmetry of SiC_3 (Fig. 1) is confirmed by (i) the absence of transitions between levels with odd K, and (ii) the hyperfine pattern in the FTM spectrum of the disubstituted off-axis ^{13}C isotopic species which shows that the two carbon atoms are equivalent. Comparison of the full set of spectroscopic constants with those of other molecules shows that the fourth-order centrifugal distortion constants (Table IV) are intermediate between those of the cumulene carbenes H_2CCC (Ref. 10) and H_2CCCC (Ref. 13), confirming that SiC_3 is fairly rigid because the distortion constants scale with reduced mass μ roughly as μ^{-2}.

A. Molecular structure

The structure of SiC_3 was obtained by a least-squares adjustment of the three bonds in Fig. 1 to reproduce, by means of the Hamiltonian for rigid body rotation, the measured transitions of the six isotopic species (Table I) on the assumption that rhomboidal SiC_3 is planar and has C_{2v} symmetry. The bond lengths in the zero-point (r_0) structure (Fig. 1) are compared in Table VI with equilibrium r_e structures calculated *ab initio* at four levels of theory: Møller–Plesset second order perturbation theory (MP2), configuration interaction with all single- and double-excitations (CISD), and couple cluster theory with single and double excitations (CCSD), and perturbative triple excitations [CCSD(T)].

In all four theoretical structures, the external bonds agree with the experimental r_0 structure to within about 0.01 Å, but the transannular bond differs from the measured bond length by 0.015–0.020 Å in the MP2, CISD, and CCSD calculations (Table VI). Only at the highest level of theory [CCSD(T)/cc-pVTZ] is the difference between the experimental and theoretical estimates of the transannular bond

TABLE V. Spectroscopic constants of SiC_3 isotopic species.

Constant[a]	$SiCCC$[b]	$^{29}SiCCC$	$^{30}SiCCC$	$SiCC^{13}C$ on-axis	$Si^{13}CCC$ off-axis	$Si^{13}C^{13}CC$ off-axis
A	37 943.76(51)	37 943.76[c]	37 943.76[c]	37 943.76[c]	36 471(3)	35 038(6)
B	6 282.904(4)	6 179.05(6)	6 081.76(6)	6 060.50(4)	6 263.629(1)	6 245.331(1)
C	5 386.868(4)	5 310.29(5)	5 238.27(6)	5 222.63(4)	5 341.704(1)	5 296.764(1)
$\Delta_J\times10^3$	1.667(4)	1.6[d]	1.6[d]	1.6[d]	1.6[d]	1.6[d]
$\Delta_{JK}\times10^3$	8.55(12)				7.0(5)	8.5(11)
Inertial defect (amu Å^2):						
Δ	0.060 52(17)	0.061	0.062	0.059	0.068	0.068

[a]Rotational and centrifugal distortion constants in MHz.
[b]See Table IV for a full set of spectroscopic constants.
[c]Constrained to value of the normal isotopic species.
[d]Scaled from Δ_J of the normal isotopic species by the ratio of the reduced masses squared.

TABLE VI. SiC_3 structures.

	Experimental	Theoretical			
Bond lengths (Å)	r_0[a]	MP2[b]	CISD[c]	CCSD[d]	CCSD(T)[d]
$r(Si–C_1)$	1.834(2)	1.846	1.825	1.830	1.840
$r(C_1–C_2)$	1.435(2)	1.441	1.438	1.427	1.435
$r(C_1–C_3)$ transannular	1.490(2)	1.504	1.469	1.468	1.486

[a]Structure that best reproduces the observed rotational transitions of the six isotopic species (see Sec. IV A). Estimated uncertainties in the last significant digit are given in parentheses.
[b]From Ref. 21.
[c]From Ref. 8.
[d]From Ref. 22.

<0.010 Å. For molecules whose structures are known accurately (e.g., H_2CCC, H_2CCCC, HCCCN, H_2CCO, and c-C_3H_2), the C–C or C–O bonds calculated at the CCSD(T)/cc-pVTZ level usually agree to within 0.005 Å or better with those of the r_0 structure. The same close agreement between the CCSD(T) structure and experiment is observed in SiC_3. Nevertheless, even at the MP2, CISD, and CCSD levels of theory, the calculated B and C rotational constants agree with the measured constants to within 1% or better. On the basis of this work, it appears that structures of fairly small silicon carbides calculated at modest levels of theory are sufficiently accurate to guide laboratory searches.

It should be feasible for quantum chemists to calculate the vibration–rotation coupling constants (α_i) and obtain an accurate experimental/theoretical equilibrium structure by converting the measured rotational constants to equilibrium constants. Calculation of the coupling constants requires computation of the cubic force field, which in turn may provide insight into the nature of the unusual bonding in rhomboidal SiC_3.

V. DISCUSSION

The lines of rhomboidal SiC_3 are among the strongest observed for a reactive species with the present FTM spectrometer, and it would be surprising if other silicon-containing organic molecules could not be found. Six, in fact, were detected while the present analysis was underway. Two of these are isomers of the present ring, each calculated to lie about 5 kcal higher in energy:[8] one a linear chain with a triplet electronic ground state, the second a singlet rhomboid ring with the same C_{2v} symmetry as here. The remaining four are linear carbon chains: SiC_5 and SiC_7, both with triplet electronic ground states and large fine structure splittings in their rotational spectra, and SiC_6 and SiC_8, both singlet closed shell molecules.[2] A full account of these silicon–carbon molecules, none of which to our knowledge has previously been observed spectroscopically or otherwise, will appear elsewhere. It is likely that other rings and chains of similar composition, perhaps significantly larger ones, remain to be discovered.

Because SiC, SiC_2, and SiC_4 have been detected in at least one astronomical source (the expanding circumstellar shell of the carbon star IRC+10 216; Refs. 7,14,15), a search for SiC_3 was undertaken with a radio telescope as soon as its millimeter-wave spectrum was in hand (Tables III and IV). Seven lines were quickly detected at precisely the expected frequencies, establishing SiC_3 as the largest cyclic molecule by size and mass to be identified in space to date.[2] The number of lines measured so far is not adequate to determine the rotational excitation and partition function very accurately, but it is already clear that the excitation of SiC_3 is quite similar to that of SiC_2, a molecule with similar symmetry. The rotational temperature is again low (13 K) within the K ladders, owing to rapid radiative decay, but high (46 K) across them, because cross-ladder radiative transitions are forbidden. Our current estimate of the column density of SiC_3 in the circumstellar shell of IRC+10 216, 4×10^{12} cm^{-2}, is probably uncertain by a factor of 2 or more owing to uncertainty in the rotational partition function, and could be significantly tightened by detection of more of the transitions listed in the Appendix.

The density of SiC_3 in our supersonic beam, estimated to be about 3×10^8 cm^{-3}, is high by the standards of laser spectroscopy, so visible or ultraviolet electronic transitions may be detectable. The somewhat similar SiC_2 ring has a strong transition in the blue–green near 498 nm ($^1B_2–X\ ^1A_1$; the Merrill–Sanford bands long known in stellar spectra) which is readily observed by laser-induced fluorescence,[16] cavity ring-down laser absorption spectroscopy,[17] and resonant enhanced two-photon ionization.[18] Rhombic C_4, isovalent with SiC_3 here, is predicted to have an allowed transition near 530 nm ($^1B_1–X\ ^1A_1$), with a fairly high oscillator strength ($f\sim0.02$; Refs. 19,20); the analogous transition in SiC_3 may be detectable both in the laboratory and in space when the approximate wavelength has been estimated by quantum chemists.

With the construction of a new receiver and other refinements, the spectral range of the FTM spectrometer was extended to nearly 40 GHz after the present work was completed. Three new lines of SiC_3 were measured near 35 GHz, and found to lie almost exactly at the frequencies predicted with the constants in Table IV. These are the single $J=3–2$ transition in the $K=0$ ladder, and the two $J=3–2$ transitions in the $K=2$ ladder. From the intensities of the $K=2$ lines relative to that of $K=0$, the rotational temperature of SiC_3 is estimated to be about 1.5 K.

ACKNOWLEDGMENTS

We wish to thank H. F. Schaefer III, T. D. Crawford, J. F. Stanton, and W. Klemperer for valuable advice during the course of this work, and J. K. G. Watson for a critical reading of the manuscript.

APPENDIX

The most intense R-branch transitions of SiC_3 can be predicted up to 300 GHz to high accuracy with the spectroscopic constants in Table IV. In the accompanying table of predicted frequencies (Table VII), the $K=0$ lines should be the most accurate, because the two lowest $K=0$ transitions were measured at centimeter wavelengths in addition to 12 millimeter-wave lines. On the other hand, the estimated uncertainties of the $K=6$, and 8 transitions are several times

TABLE VII. Predicted frequencies of SiC_3 calculated from the spectroscopic constants in Table IV. Estimated uncertainties (in parentheses) are 1σ in the last significant digit. S is the asymmetric rotor line strength and E/k is the energy of the upper level of the transition. Transitions labeled with only one K subscript indicate a closely spaced doublet whose separation is <1.3 km s^{-1}. Lines included in the table are those with $K \leqslant 8$ and $E \leqslant 175$ K; lines between 50–69 GHz and 179–189 GHz are omitted owing to high atmospheric opacity.

Frequency	Transition	S	E/k (K)	Frequency	Transition	S	E/k (K)
11669.766(1)	$1_{0,1}\rightarrow 0_{0,0}$	1.00	0.6	163528.62(52)	$14_8\rightarrow 13_8$	9.43	157.5
23320.744(2)	$2_{0,2}\rightarrow 1_{0,1}$	2.00	1.7	163640.51(13)	$14_6\rightarrow 13_6$	11.43	114.3
34934.204(3)	$3_{0,3}\rightarrow 2_{0,2}$	3.00	3.4	163949.12(2)	$14_{4,11}\rightarrow 13_{4,10}$	12.86	83.6
35008.937(4)	$3_{2,2}\rightarrow 2_{2,1}$	1.67	9.5	163999.82(2)	$14_{4,10}\rightarrow 13_{4,9}$	12.86	83.6
35083.870(5)	$3_{2,1}\rightarrow 2_{2,0}$	1.67	9.5	167684.64(1)	$15_{0,15}\rightarrow 14_{0,14}$	14.93	65.5
46491.690(4)	$4_{0,4}\rightarrow 3_{0,3}$	4.00	5.6	168324.95(2)	$14_{2,12}\rightarrow 13_{2,11}$	13.72	66.1
46663.823(5)	$4_{2,3}\rightarrow 3_{2,2}$	3.00	11.8	173372.09(1)	$15_{2,14}\rightarrow 14_{2,13}$	14.72	73.0
46850.794(6)	$4_{2,2}\rightarrow 3_{2,1}$	3.00	11.8	175227.80(54)	$15_8\rightarrow 14_8$	10.73	165.9
69369.99(1)	$6_{0,6}\rightarrow 5_{0,5}$	5.99	11.7	175365.14(12)	$15_6\rightarrow 14_6$	12.60	122.8
69932.52(1)	$6_{2,5}\rightarrow 5_{2,4}$	5.33	17.9	175735.70(2)	$15_{4,12}\rightarrow 14_{4,11}$	13.93	92.0
70079.45(2)	$6_4\rightarrow 5_4$	3.33	36.4	175818.16(2)	$15_{4,11}\rightarrow 14_{4,10}$	13.93	92.0
70579.63(1)	$6_{2,4}\rightarrow 5_{2,3}$	5.33	18.0	178362.04(1)	$16_{0,16}\rightarrow 15_{0,15}$	15.93	74.0
80662.34(1)	$7_{0,7}\rightarrow 6_{0,6}$	6.99	15.6	189040.57(1)	$17_{0,17}\rightarrow 16_{0,16}$	16.93	83.1
81540.07(1)	$7_{2,6}\rightarrow 6_{2,5}$	6.43	21.8	192883.49(2)	$16_{2,14}\rightarrow 15_{2,13}$	15.76	84.0
81735.20(9)	$7_6\rightarrow 6_6$	1.86	71.2	195958.33(2)	$17_{2,16}\rightarrow 16_{2,15}$	16.74	91.3
81777.73(2)	$7_4\rightarrow 6_4$	4.71	40.3	198837.39(11)	$17_6\rightarrow 16_6$	14.88	141.3
82563.53(1)	$7_{2,5}\rightarrow 6_{2,4}$	6.43	21.9	199343.22(1)	$17_{4,14}\rightarrow 16_{4,13}$	16.06	110.6
91844.84(1)	$8_{0,8}\rightarrow 7_{0,7}$	7.98	20.0	199540.67(1)	$17_{4,13}\rightarrow 16_{4,12}$	16.06	110.6
93125.63(1)	$8_{2,7}\rightarrow 7_{2,6}$	7.50	26.3	199725.52(1)	$18_{0,18}\rightarrow 17_{0,17}$	17.93	92.7
93421.57(10)	$8_6\rightarrow 7_6$	3.50	75.6	205073.36(2)	$17_{2,15}\rightarrow 16_{2,14}$	16.78	93.9
93484.52(2)	$8_4\rightarrow 7_4$	6.00	44.8	207187.90(1)	$18_{2,17}\rightarrow 17_{2,16}$	17.75	101.3
94634.68(1)	$8_{2,6}\rightarrow 7_{2,5}$	7.50	26.5	210419.56(2)	$19_{0,19}\rightarrow 18_{0,18}$	18.93	102.8
102916.13(1)	$9_{0,9}\rightarrow 8_{0,8}$	8.97	24.9	210586.07(10)	$18_6\rightarrow 17_6$	16.00	151.4
104686.17(1)	$9_{2,8}\rightarrow 8_{2,7}$	8.55	31.3	211161.68(1)	$18_{4,15}\rightarrow 17_{4,14}$	17.11	120.7
105081.36(39)	$9_8\rightarrow 8_8$	1.89	123.8	211454.51(1)	$18_{4,14}\rightarrow 17_{4,13}$	17.11	120.8
105111.91(11)	$9_6\rightarrow 8_6$	5.00	80.7	217186.04(2)	$18_{2,16}\rightarrow 17_{2,15}$	17.79	104.3
105199.98(2)	$9_{4,6}\rightarrow 8_{4,5}$	7.22	49.9	218374.97(1)	$19_{2,18}\rightarrow 18_{2,17}$	18.76	111.7
105202.08(2)	$9_{4,5}\rightarrow 8_{4,4}$	7.22	49.9	221123.55(2)	$20_{0,20}\rightarrow 19_{0,19}$	19.92	113.4
106791.03(1)	$9_{2,7}\rightarrow 8_{2,6}$	8.56	31.6	222343.84(10)	$19_6\rightarrow 18_6$	17.11	162.1
113882.03(1)	$10_{0,10}\rightarrow 9_{0,9}$	9.96	30.4	222987.46(1)	$19_{4,16}\rightarrow 18_{4,15}$	18.16	131.4
124755.05(1)	$11_{0,11}\rightarrow 10_{0,10}$	10.96	36.4	223411.12(1)	$19_{4,15}\rightarrow 18_{4,14}$	18.16	131.5
127720.67(1)	$11_{2,10}\rightarrow 10_{2,9}$	10.63	43.0	229210.83(2)	$19_{2,17}\rightarrow 18_{2,16}$	18.80	115.3
128451.56(45)	$11_8\rightarrow 10_8$	5.18	135.6	229520.08(1)	$20_{2,19}\rightarrow 19_{2,18}$	19.76	122.7
128506.46(12)	$11_6\rightarrow 10_6$	7.73	92.5	231837.23(2)	$21_{0,21}\rightarrow 20_{0,20}$	20.92	124.5
128663.76(2)	$11_{4,8}\rightarrow 10_{4,7}$	9.55	61.7	234111.24(9)	$20_6\rightarrow 19_6$	18.20	173.3
128672.82(2)	$11_{4,7}\rightarrow 10_{4,6}$	9.55	61.7	234818.03(1)	$20_{4,17}\rightarrow 19_{4,16}$	19.20	142.7
131315.17(2)	$11_{2,9}\rightarrow 10_{2,8}$	10.64	43.6	235417.21(1)	$20_{4,16}\rightarrow 19_{4,15}$	19.20	142.8
135552.63(2)	$12_{0,12}\rightarrow 11_{0,11}$	11.95	42.9	240624.27(1)	$21_{2,20}\rightarrow 20_{2,19}$	20.77	134.3
139189.20(1)	$12_{2,11}\rightarrow 11_{2,10}$	11.66	49.7	241138.05(2)	$20_{2,18}\rightarrow 19_{2,17}$	19.80	126.9
140140.75(48)	$12_8\rightarrow 11_8$	6.67	142.3	242559.68(2)	$22_{0,22}\rightarrow 21_{0,21}$	21.92	136.2
140211.68(13)	$12_6\rightarrow 11_6$	9.00	99.2	246650.40(1)	$21_{4,18}\rightarrow 20_{4,17}$	20.24	154.5
140413.15(2)	$12_{4,9}\rightarrow 11_{4,8}$	10.67	68.4	247480.05(1)	$21_{4,17}\rightarrow 20_{4,16}$	20.24	154.7
140430.08(2)	$12_{4,8}\rightarrow 11_{4,7}$	10.67	68.4	251689.08(1)	$22_{2,21}\rightarrow 21_{2,20}$	21.77	146.4
143645.36(2)	$12_{2,10}\rightarrow 11_{2,9}$	11.67	50.5	252958.60(2)	$21_{2,19}\rightarrow 20_{2,18}$	20.80	139.0
146294.46(1)	$13_{0,13}\rightarrow 12_{0,12}$	12.94	49.9	253289.74(2)	$23_{0,23}\rightarrow 22_{0,22}$	22.92	148.3
150621.98(1)	$13_{2,12}\rightarrow 12_{2,11}$	12.68	56.9	258481.06(1)	$22_{4,19}\rightarrow 21_{4,18}$	21.27	166.9
151833.02(50)	$13_8\rightarrow 12_8$	8.08	149.6	259607.18(1)	$22_{4,18}\rightarrow 21_{4,17}$	21.27	167.1
151922.86(13)	$13_6\rightarrow 12_6$	10.23	106.5	262716.46(2)	$23_{2,22}\rightarrow 22_{2,21}$	22.78	159.0
152174.88(2)	$13_{4,10}\rightarrow 12_{4,9}$	11.77	75.7	264026.14(1)	$24_{0,24}\rightarrow 23_{0,23}$	23.92	161.0
152204.86(2)	$13_{4,9}\rightarrow 12_{4,8}$	11.77	75.7	264663.66(3)	$22_{2,20}\rightarrow 21_{2,19}$	21.80	151.7
155989.88(2)	$13_{2,11}\rightarrow 12_{2,10}$	12.70	58.0	273708.71(2)	$24_{2,23}\rightarrow 23_{2,22}$	23.78	172.1
156999.66(1)	$14_{0,14}\rightarrow 13_{0,13}$	13.94	57.4	274767.71(2)	$25_{0,25}\rightarrow 24_{0,24}$	24.92	174.2
162016.87(1)	$14_{2,13}\rightarrow 13_{2,12}$	13.70	64.7	276244.91(4)	$23_{2,21}\rightarrow 22_{2,20}$	22.80	164.9

greater than those of the $K=0$, 2, and 4 transitions ($\sim$0.1 ppm), because only two $K=6$ doublets were observed in the millimeter-wave band and $K=8$ transitions were not measured. Nevertheless, the calculated frequencies for $K \leqslant 6$ should be sufficiently accurate for future astronomical observations since lines in the molecular envelope of IRC+10216 are quite broad (FWHM$\sim$29 km s^{-1}) and uncertainties in rest frequencies derived from even the most intense astronomical features are typically $\geqslant$1 ppm in this source.

[1] M. C. McCarthy, A. J. Apponi, and P. Thaddeus, J. Chem. Phys. **110**, 10645 (1999).
[2] A. J. Apponi, M. C. McCarthy, C. A. Gottlieb, and P. Thaddeus, Astrophys. J. Lett. **516**, L103 (1999).
[3] M. C. McCarthy, M. J. Travers, A. Kovács, C. A. Gottlieb, and P. Thaddeus, Astrophys. J., Suppl. Ser. **113**, 105 (1997).
[4] R. Mollaaghababa, C. A. Gottlieb, and P. Thaddeus, J. Chem. Phys. **98**, 968 (1993).
[5] M. C. McCarthy, C. A. Gottlieb, A. L. Cooksy, and P. Thaddeus, J. Chem. Phys. **103**, 7779 (1995).
[6] C. A. Gottlieb, J. M. Vrtilek, and P. Thaddeus, Astrophys. J. Lett. **343**, L29 (1989).
[7] J. Cernicharo, C. A. Gottlieb, M. Guélin, P. Thaddeus, and J. M. Vrtilek, Astrophys. J. Lett. **341**, L25 (1989).
[8] I. L. Alberts, R. S. Grev, and H. F. Schaefer III, J. Chem. Phys. **93**, 5046 (1990).
[9] *Matheson Gas Data Book* (Matheson, East Rutherford, NJ, 1966).
[10] C. A. Gottlieb, T. C. Killian, P. Thaddeus, P. Botschwina, J. Flügge, and M. Oswald, J. Chem. Phys. **98**, 4478 (1993).
[11] I. M. B. Nielsen, W. D. Allen, A. G. Császár, and H. F. Schaefer III, J. Chem. Phys. **107**, 1195 (1997).
[12] W. Gordy, and R. L. Cook, *Microwave Molecular Spectra* (Wiley, New York, 1984), p. 687.
[13] T. C. Killian, J. M. Vrtilek, C. A. Gottlieb, E. W. Gottlieb, and P. Thaddeus, Astrophys. J. Lett. **365**, L89 (1990).
[14] P. Thaddeus, S. E. Cummins, and R. A. Linke, Astrophys. J. Lett. **283**, L45 (1984).
[15] M. Ohishi, N. Kaifu, K. Kawaguchi, A. Murakami, S. Saito, S. Yamamoto, S. Ishikawa, Y. Fujita, Y. Shiratori, and W. M. Irvine, Astrophys. J. Lett. **345**, :L83 (1989).
[16] T. J. Butenhoff and E. A. Rohlfing, J. Chem. Phys. **95**, 1 (1991).
[17] C. D. Ball, personal communication (1999).
[18] D. L. Michalopoulos, M. E. Geusic, P. R. R. Langridge-Smith, and R. E. Smalley, J. Chem. Phys. **80**, 3556 (1984).
[19] J. F. Stanton and R. J. Bartlett, J. Chem. Phys. **98**, 7029 (1993).
[20] H. Koch, R. Kobayashi, A. S. de Merás, and P. Jørgensen, J. Chem. Phys. **100**, 4393 (1994).
[21] M. Gomei, R. Kishi, A. Nakajima, S. Iwata, and K. Kaya, J. Chem. Phys. **107**, 10051 (1997).
[22] T. D. Crawford (personal communication).